HISTOLOGICAL, IMMUNOHISTOCHEMICAL, AND MOLECULAR EXAMINATION OF THE PATHOMECHANISMS OF ATRIAL FIBRILLATION

PhD thesis – short version

Szilvia Kugler, MD

Doctoral School of Theoretical and Translational Medicine,
Semmelweis University

Supervisors: Tamás Radovits, MD, Ph.D
Ágnes Nemeskéri, MD, Ph.D

Official reviewers: Márton Ákos Lőrincz, MD, Ph.D
Zoltán Husti, MD, Ph.D

Head of the Complex Examination Committee:
István Karádi, MD, Ph.D

Members of the Complex Examination Committee:
Henriette Farkas, MD, Ph.D; Péter Andréka, MD, Ph.D

Budapest
2025

1. INTRODUCTION

Atrial fibrillation (AF) has a major impact on health care due to the substantial mortality and morbidity associated with heart failure (HF) and ischemic stroke. AF is presumed to be induced by focal electrical activations that usually originate from the myocardial sleeves (MSs) of the pulmonary veins (PVs) or less often from the superior vena cava (SVC), inferior vena cava (IVC) or coronary sinus (CS). Cardiomyocytes with pacemaker cell and Purkinje fiber morphology were found in the MSs of human PVs, but no similar cells were documented in human caval veins and CS. Connexin 45 (Cx45) is a specific marker of the pacemaker and conduction system, whereas Cx43 is present in the working myocardium. Cx45 may help to identify conducting-like cardiomyocytes in the venous MSs, however, human data are lacking. Desmin intermediate filament has also been reported to be abundant in the pacemaker and conduction system, in contrast to the weaker labeling of the working myocardium.

Structural remodeling of the atria (for example atrial fibrosis, amyloid deposits or lymphomononuclear infiltrates) is essential for the persistence of AF. Elevated levels of inflammatory cytokines (interleukin (IL)-1, IL-6) were detected in blood samples of AF patients compared to those in sinus rhythm (SR). Inflammasome complexes have been shown to play a role in the initiation and maintenance of AF. The activation of inflammasomes requires a priming event that induces the synthesis of “NLR family, pyrin domain containing 3” (NLRP3) and pro-IL-1β, and a subsequent trigger signal that promote the assembly of NLRP3, “apoptosis-associated speck-like protein containing a CARD”

(ASC) and precursor caspase-1, resulting in active caspase-1 that cleaves and activates pro-IL-1β. In addition to the NLRP3, other inflammasome pathways, namely "NLR family, pyrin domain containing 1" (NALP1), "NLR family CARD domain-containing protein 4" (NLRC4) and "absent in melanoma 2" (AIM2) have been identified to play a role in cardiovascular diseases.

HF is a known risk factor for AF. However, numerous patients suffering from HF never develop AF, suggesting pathological differences between HF with AF and HF with SR. Serum levels of some inflammatory markers (for example IL-6) proved to be higher in HF patients with AF than in HF patients with SR, suggesting that inflammatory mechanisms may play a role in HF-associated AF.

2. OBJECTIVES

2.1. We aimed to examine whether the MSs ensheathing the SVC, IVC, PVs and CS contain any cardiomyocytes possessing the conducting phenotype. We targeted Cx45 and desmin.

2.2. We aimed to assess whether there is a role for inflammasome activation, macrophage infiltration or fibrosis in HF-associated AF.

3. METHODS

3.1. Histological and immunohistochemical examinations of the myocardial sleeves around cardiac veins

3.1.1. Human tissues

Forty-three adult (9/43 cases with known clinical data) and a 23-week-old fetal heart were analyzed. PVs were investigated in 26/44, SVC in

35/44, IVC in 18/44 and CS in 19/44 cases. Tissue samples were also obtained from the sinoatrial node (SAN), atria and ventricles. The work was approved by the Regional and Institutional Committee of Science and Research Ethics, Semmelweis University (No. 122/2016) and the Research Ethics Committee of the Medical Research Council of Hungary (No. IV/1555-1/2021/EKU).

3.1.2. Histological staining and immunohistochemistry

Sections were stained with hematoxylin-eosin and Krutsay's trichrome. Specific stainings were performed to demonstrate glycogen (Best's Carmine), muscle striations (Heidenhain's iron hematoxylin) and amyloid (Congo red). Cx45 immunostaining was performed on ethanol-fixed samples of 3 hearts. Cx43 immunohistochemistry was performed on the frozen sections of one heart. Cx45 was detected using a rabbit polyclonal antibody (Santa Cruz Biotechnology Inc; Cat# sc-25716; dilution 1:50-1:100), and Cx43 was detected using a goat polyclonal antibody (Santa Cruz; Cat# sc-6560; dilution 1:50). Desmin immunohistochemistry was performed on formaldehyde- or ethanol-fixed samples of 16 hearts. Desmin was detected using a mouse monoclonal antibody (Dako; Cat# M0760; dilution 1:4000-1:5000 for ethanol-fixed hearts and 1:200-1:400 for formaldehyde-fixed hearts). For Cx45-desmin double immunofluorescence staining, Cx45 was detected using a rabbit polyclonal antibody (Santa Cruz; Cat# sc-25716; dilution 1:50), while desmin was detected using a mouse monoclonal antibody (Dako; Clone D33; Cat# M0760; dilution 1:5000). The intensity of desmin immunostaining was assessed using ImageJ 1.51 k

(NIH, Bethesda, MD, US) for the following structures of 4 hearts: ventricular conduction system and working myocardium, SAN, SVC, PV, CS. Signal intensity of the strongly immunoreactive cells of the conducting system and the MSs was compared with that of weaker labeled working cardiomyocytes. Differences between signal intensity at representative areas of the conduction system or MSs and the working myocardium were also investigated. For statistical analyses, a mixed effect regression model and Tukey method adjustment were used.

3.2. Investigation of inflammasome activation in end-stage heart failure-associated atrial fibrillation

3.2.1. Human samples

Left atrial samples from explanted hearts of 24 patients with end-stage ischemic HF undergoing heart transplantation were obtained from the Transplantation Biobank of the Heart and Vascular Center, Semmelweis University. The samples were immediately snap frozen in liquid nitrogen after excision. Formalin-fixed, paraffin-embedded tissues were also prepared. The project was approved by the Institutional and National Ethics Committee (ETT TUKEB 7891/2012/EKU (119/PI/12.) and ETT TUKEB IV/10161-1/2020). Twelve patients had no AF (SR group) and twelve patients had persistent or permanent AF (AF group, n=12). All individuals were male between 43-64 years of age.

3.2.2. Assessment of inflammasome activation

The expression of inflammasome sensors (NALP1, NLRP3, AIM2, NLRC4) and their downstream signaling (ASC, caspase-1, cleaved

caspase-1, IL-1β, cleaved IL-1β) were analyzed by Western blot. The following primary antibodies (Cell Signaling) were used (dilution in parenthesis): NALP1: Cat# 4990S (1:2500); NLRP3: Cat# 15101S (1:2500); AIM2: Cat# 12948S (1:2500); NLRC4: Cat# 12421S (1:2500); ASC: Cat# 13833S (1:5000); caspase-1: Cat# 3866S (1:1000); cleaved caspase-1: Cat# 4199S (1:1000); IL-1β: Cat# 12703S (1:1000); cleaved IL-1β: Cat# 83186S (1:1000). Five samples (2 from the SR group and 3 from the AF group) were excluded from analysis due to low-quality homogenates. Glyceraldehyde-3-phosphate dehydrogenase (GAPDH) was used as a loading control.

3.2.3. Assessment of macrophage infiltration

To assess the presence of macrophages in the epicardium and myocardium of left atrial samples from the SR and AF groups, immunohistochemistry was performed to detect ionized calcium-binding adaptor molecule 1 (Iba1) using a rabbit polyclonal antibody (Fujifilm Wako; Cat# 019-19741; dilution 1:2000). Macrophages were counted at several unit areas by the ImageJ 1.51 k program and averaged for the sample. Myocardial and epicardial regions were investigated separately. Data were normalized to the mean values of the SR group.

3.2.4. Evaluation of fibrosis

Analysis of fibrosis was performed on Masson's trichrome-stained samples by the ImageJ 1.51 k program. The percentage of total fibrosis was defined as the amount of fibrotic areas compared to the whole area of the section. The percentage of interstitial fibrosis was measured by correlating the amount of interstitial fibrosis to a modified area of the

section. In case of both the fibrotic and reference area for interstitial fibrosis calculation, the epicardium, subepicardial fibrotic region and perivascular fibrosis were removed at the beginning of the analysis.

3.2.5. Statistical analysis

Comparisons of two groups were performed using unpaired Student's t-test (in case of normal distribution) or Mann-Whitney test (in case of non-normal distribution). The Shapiro-Wilk test was used to test normality. Correlation and regression analysis was used to evaluate the correlations of cleaved caspase-1 with other inflammasome markers. Outlier analysis was performed by ROUT test (Q = 1%). All analyses were conducted using GraphPad Prism 8. (GraphPad Software Inc). We considered a P-value of <0.05 to be statistically significant.

4. RESULTS

4.1. Histology of the cardiac pacemaker and conduction system

In the SAN, small pacemaker cells embedded in fibrous connective tissue were observed around and in the adventitial layer of the sinoatrial nodal artery (Figure 1.A). Purkinje fibers with pale cytoplasm and peripheral myofibrils were found in the ventricular conduction system (Figure 1.B). Prominent Cx45 labeling was detected in the SAN and in the ventricular conduction system. In contrast, the ventricular working myocardium lacked the Cx45 signal. Cx43 immunoreaction was marked throughout the working myocardium. Both pacemaker cells of the SAN and Purkinje fibers exhibited strong desmin immunoreactivity compared to the weaker labeling of the working myocardium.

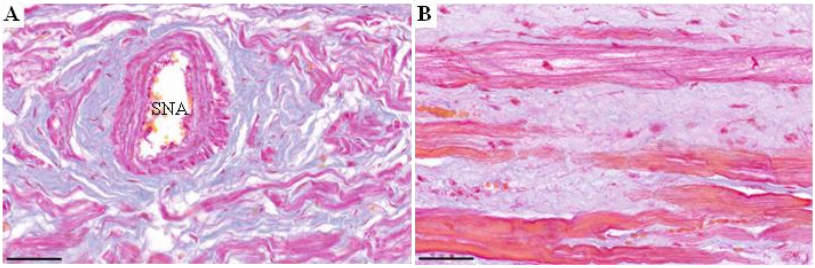

Figure 1. The cardiac pacemaker and conduction system.

SNA: sinoatrial nodal artery. Trichrome. Scale bar: 50 μm

4.2. Myocardial sleeves of the pulmonary veins

MS was identified around 92% of the left superior, 88% of the left inferior, 80% of the right superior and 100% of the right inferior PVs (Figure 2.A,B). Cardiomyocytes exhibiting Purkinje-like (Figure 2.C) or pacemaker cell-like morphology embedded in a network of fine dense connective tissue were identified in 77% of the left superior, 65% of the left inferior, 60% of the right superior and 42% of the right inferior PVs. Small SAN-like structures (Figure 2.D) were identified in 2 PVs. Best's Carmine stain revealed the presence of glycogen-rich cardiomyocytes (Figure 2.E). Special cardiomyocytes were present in young and old patients as well, regardless of their medical history. Prominent Cx45 (Figure 2.F) and desmin (Figure 2.G) labeling was detected. Double immunofluorescence staining for desmin (red) and Cx45 (green) showed a strong sarcomeric and junctional pattern for desmin labeling. Intense Cx45 immunoreactivity was restricted to the intercalated discs where it overlapped extensively with desmin (yellow; Figure 2.H). In an 86-year-old female patient, amyloid was observed in the vessel walls and MSs of all four PVs.

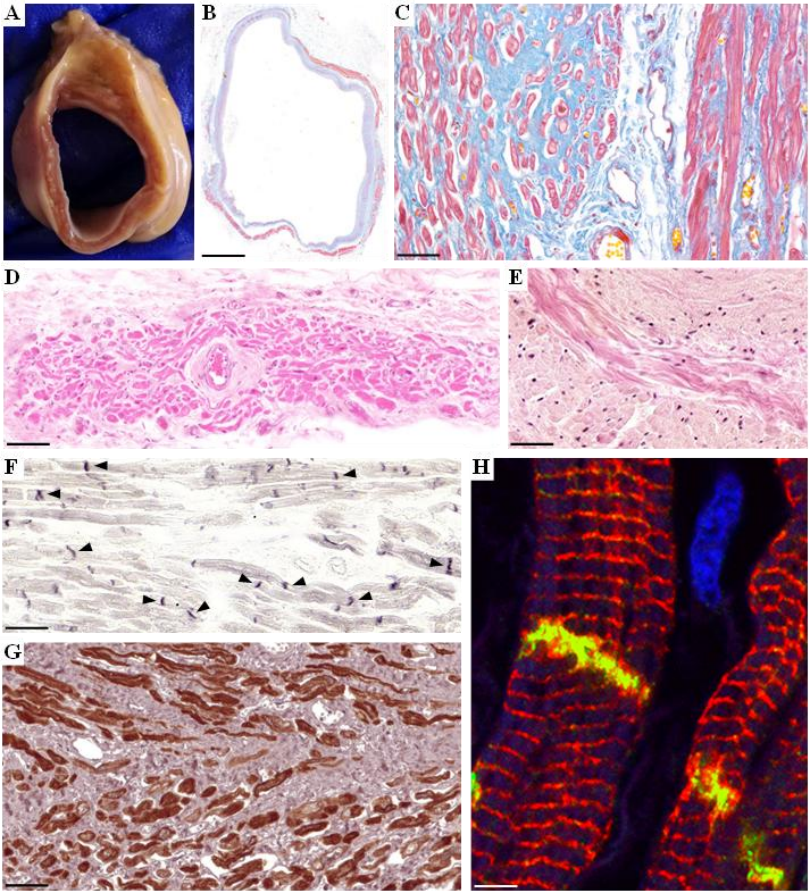

Figure 2. Myocardial sleeves of the pulmonary veins.

Trichrome (B, C), hematoxylin-eosin (D), Best's carmine (E), Cx45 (F), desmin (G), Cx45+desmin (H). Scale bar: 2000 μm (B), 50 μm (C, G), 60 μm (D, E), 45 μm (F), 10 μm (H)

4.3. Myocardial sleeve of the caval veins and coronary sinus

MSs were found around 100% of the SVCs, 78% of the IVCs and 100% of the CSs. Purkinje-like cardiomyocytes and pacemaker cells were

observed in 88% of the SVCs, 78% of the IVCs and 89% of the CSs. Special cardiomyocytes were present in young and old patients as well, both with cardiac disease and with no medical history. In SVC and CS, Cx45 labeling was prominent, while Cx43 immunoreaction proved to be weak. MSs of SVC and CS samples were frequently strongly immunopositive for desmin. In an 86-year-old female patient, amyloid deposits were observed in the vessel wall of the SVC, in the MS of the IVC and both in the vessel wall and in the MS of the CS. In a 54-year-old female patient, we identified a small SAN-like structure in the MS of the distal SVC. In three CS samples, small SAN-like structures were identified in the middle part of the vessel. One of these was a 22-year-old female for whom we detected thin cardiomyocytes in the adventitia of a small artery and in the connective tissue around the artery (Figure 3.A,B). Heidenhain's iron hematoxylin stain confirmed muscle striations inside the pacemaker cell-like cardiomyocytes (Figure 3.C).

4.4. Quantitative analysis of desmin immunostaining

Pooled analysis of cells from 4 hearts showed significantly stronger desmin signal intensity for Purkinje fibers, pacemaker cells and highly immunoreactive cardiomyocytes of the venous MSs compared to the ventricular working cardiomyocytes. Although less immunoreactive cardiomyocytes were also present in the MSs, desmin signal intensity proved to be significantly stronger in all venous MSs than in ventricular working myocardium during pooled analysis of representative areas. Due to the extensive connective tissue, signal intensity of the SAN did not differ from that of the working myocardium (Figure 4).

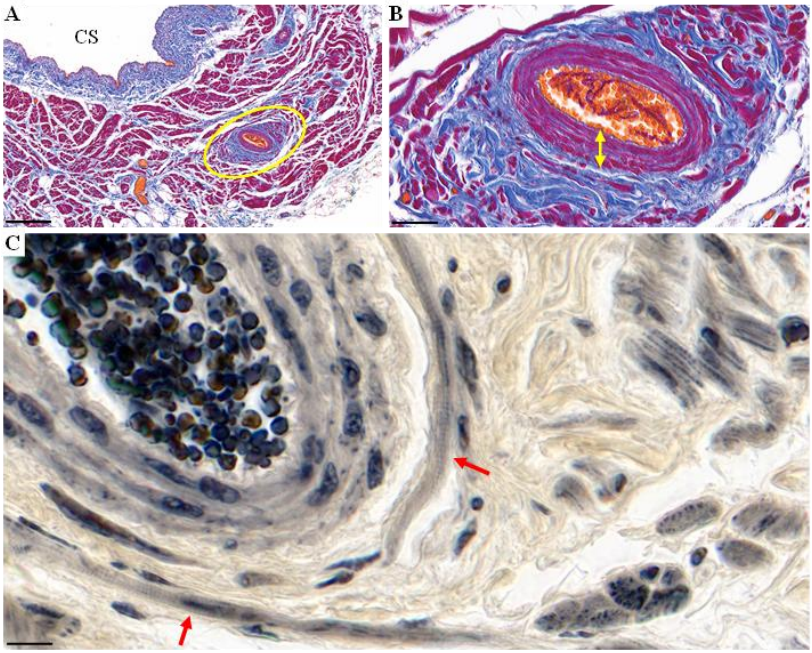

Figure 3. Sinoatrial node-like structure around the coronary sinus. *Yellow circle: SAN-like structure (A). Double arrow: tunica media of the small artery (B). Arrows: small cardiomyocytes in the adventitia of the artery (C). Trichrome (A, B), Heidenhain's iron hematoxylin (C). Scale bar: 200 μm (A), 35 μm (B), 11 μm (C)*

4.5. Histological features of the human fetal heart

Myocardial extensions into the SVC could be observed in the 23-week-old human fetus. Prominent desmin labeling was detected in the MS of the SVC and at the SAN region. Cx45 immunoreaction was intense in the cells around the sinoatrial nodal artery and in the MS of the SVC.

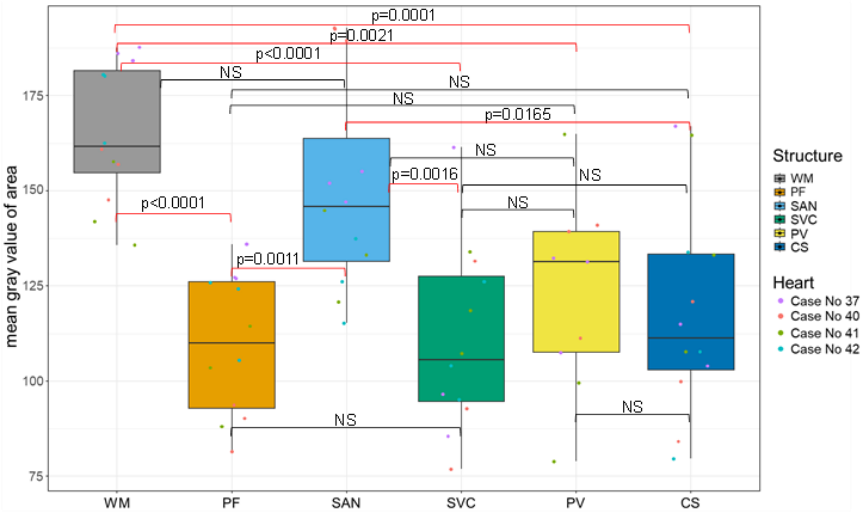

Figure 4. Pooled analysis of areas from 4 hearts for desmin labeling

Lower mean gray value indicates stronger desmin signal intensity. Medians, first and third quartiles, minimum and maximum values are presented for each structure. CS: coronary sinus; NS: non significant; PF: Purkinje fibers; PV: pulmonary vein; SAN: sinoatrial node; SVC: superior vena cava; WM: ventricular working myocardium

4.6. Inflammation in heart failure-associated atrial fibrillation

4.6.1. Inflammasome activation

No significant differences were observed in the expression of any inflammasome sensors between the AF and SR groups. There was a strong tendency that protein expression of cleaved caspase-1 was increased in the AF versus SR group (p=0.051). Cleaved caspase-1 was correlated with interleukin-1β and its cleaved form in both the total population (p=0.005 and 0.004, respectively) and the AF group

(p=0.01), but not in the SR group, indicating the presence of inflammation in AF patients. No correlation was found with any inflammasome sensors, suggesting a primary effect on inflammasome activity rather than on inflammasome priming (Figure 5).

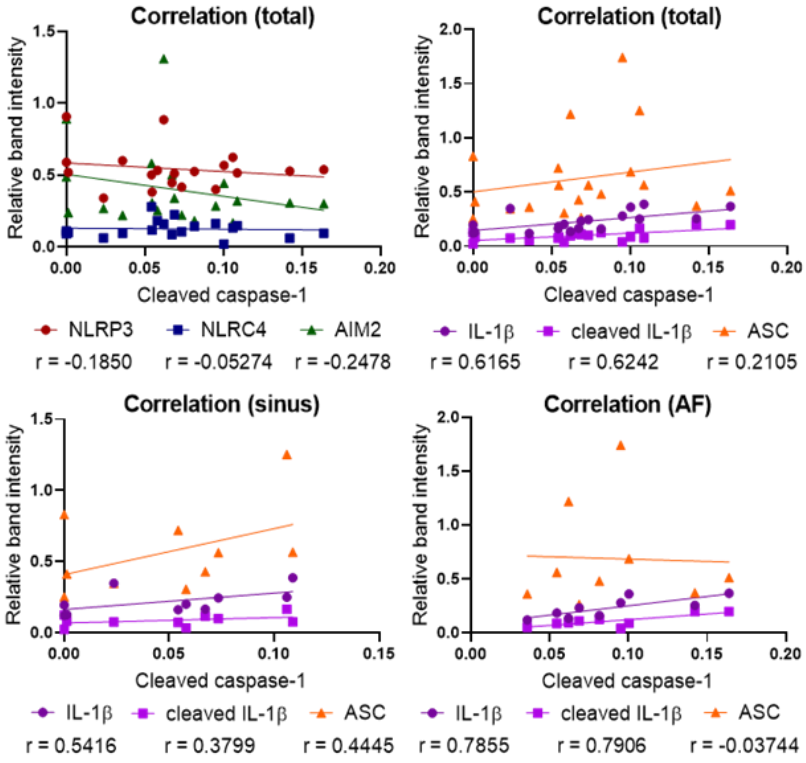

Figure 5. Inflammasome activation in heart failure-associated atrial fibrillation.

Pearson-correlation; n=9-10. p>0.05 in the sinus rhythm group and for NLRP3, NLRC4, AIM2 and ASC. p<0.05 for IL-1β and its cleaved form in the total population and in the atrial fibrillation (AF) group.

4.6.2. Macrophage infiltration

The average number of macrophages per unit area in both left atrial myocardium and epicardium was higher in the AF samples than in the SR group, but differences were not significant (p=0.09 for myocardial samples, p=0.21 for epicardial samples) (Figure 6).

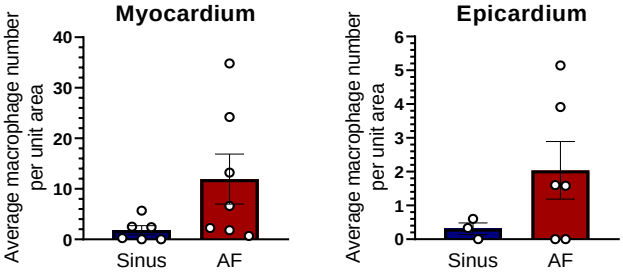

Figure 6. Macrophages in heart failure-associated atrial fibrillation.

p>0.05, Student's t-test; n=3-7. Results are expressed as mean ± standard error of the mean. AF: atrial fibrillation

4.6.3. Left atrial fibrosis

There was no difference in the percentage of either total or interstitial fibrosis between the AF and SR groups (Figure 7).

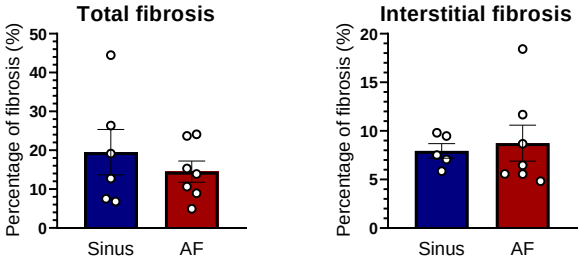

Figure 7. Atrial fibrosis in heart failure-associated atrial fibrillation.

p>0.05, Student's t-test; n=5-7. Results are expressed as mean ± standard error of the mean. AF: atrial fibrillation

5. CONCLUSIONS

In the MSs of human PVs, caval veins and CS, we found cardiomyocytes that microscopically show features of pacemaker cells and Purkinje fibers. Our research is the first to demonstrate pronounced Cx45 immunoreactivity of the MSs, which provide further support for the arrhythmogenicity of these regions. Immunostaining of desmin was stronger in the MSs than in the ventricular working myocardium. It is noteworthy that all of these observations were independent of sex, age and medical history of the patients. The prominent staining of Cx45 and desmin suggests a pacemaker and/or conducting phenotype of the venous MSs, which, however, does not always trigger arrhythmias by itself.

As a novelty, we identified SAN-like structures in 3 CS, 2 PV and 1 SVC samples. Based on the light microscopic similarity between these SAN-like structures and the true SAN, it is possible that these structures could be the source of ectopic pacemaker activity.

We investigated inflammation-related differences in failing human hearts with SR and AF, and found tendency towards increase in the expression of cleaved caspase-1 and its significant correlation with the expression of interleukin-1β and its cleaved form in the AF samples. These findings indicate that enhanced inflammasome activity (triggering) may cause AF in patients with end-stage HF. Tendentiously higher macrophage infiltration also indicates higher levels of inflammation in AF samples, while HF-associated AF seems to be independent of cardiac fibrosis.

6. BIBLIOGRAPHY OF THE CANDIDATE'S PUBLICATIONS

6.1. Publications directly related to the thesis (Σ IF=11.39)

Kugler S, Nagy N, Rácz G, Tőkés AM, Dorogi B, Nemeskéri Á. (2018) Presence of cardiomyocytes exhibiting Purkinje-type morphology and prominent connexin45 immunoreactivity in the myocardial sleeves of cardiac veins. Heart Rhythm, 15(2): 258-264. (SJR D1, IF=5.225)

Kugler S, Duray G, Préda I. (2018) Új felismerések a pitvarfibrilláció genezisében és fenntartásában: az egyénre szabott kezelés lehetőségei. Orv Hetil, 159(28): 1135-1145. (SJR Q3, IF=0.564)

Kugler S*, Onódi Z*, Ruppert M, Sayour AA, Oláh A, Benke K, Ferdinandy P, Merkely B, Radovits T, Varga ZV. (2022) Inflammasome activation in end-stage heart failure-associated atrial fibrillation. ESC Heart Fail, 9(4): 2747-2752. *Contributed equally. (SJR Q1, IF=3.8)

Kugler S, Tőkés AM, Nagy N, Fintha A, Danics K, Sághi M, Törő K, Rácz G, Nemeskéri Á. (2024) Strong desmin immunoreactivity in the myocardial sleeves around pulmonary veins, superior caval vein and coronary sinus supports the presumed arrhythmogenicity of these regions. J Anat, 244(1): 120-132. (SJR Q1, IF=1.8)

6.2. Publications not directly related to the thesis (Σ IF=16.27)

Kugler S, Pólos M, Király Á, Pataki Á, Koppányi Á, Varga T, Szakál-Tóth Z, Parázs N, Teszák T, Tarjányi Z, Prinz G, Hartyánszky I, Szabolcs Z, Merkely B, Sax B. (2021) Pseudoaneurysm of the ascending aorta: case report of a donor-derived Pseudomonas infection in a heart transplant recipient. BMC Infect Dis, 21(1): 847.

Parázs N, Lakatos BK, Kovács A, Assabiny A, Király Á, Tarjányi Z, Szakál-Tóth Z, Teszák T, Tokodi M, Ujvári A, **Kugler S**, Szücs N, Merkely B*, Sax B*. (2021) Jobbszívfél-elégtelenség évekkel a szívtranszplantációt követően: Egy ritka etiológiai tényező esete. Cardiol Hung, 51: 69-72. *Contributed equally.

Szabo D, Szabo A, Magyar L, Banhegyi G, **Kugler S**, Pinter A, Juhasz V, Ruppert M, Olah A, Ruzsa Z, Edes IF, Szekely A, Becker D, Merkely B, Hizoh I. (2022) Admission lactate level and the GRACE 2.0 score are independent and additive predictors of 30-day mortality of STEMI patients treated with primary PCI-Results of a real-world registry. PLoS One, 17(11): e0277785.

Kugler S, Vári DK, Veres DS, Király Á, Teszák T, Parázs N, Tarjányi Z, Drobni Z, Szakál-Tóth Z, Prinz G, Miheller P, Merkely B, Sax B. (2023) Seroconversion after SARS-CoV-2 vaccination is protective against severe COVID-19 disease in heart transplant recipients. Immun Inflamm Dis, 11: e1086.

Szécsi B, Sinkó R, Vereb A, Khochanskiy D, Benke K, Radovits T, Lakatos B, Kőszegi A, Losoncz E, **Kugler S**, Szabó M, Merkely B, Székely A*, Gereben B *. (2024) The perioperative period of heart transplantation is affected by thyroid hormone status. Thyroid, 34(6): 774-784. *Contributed equally.